Process diagnostics for co-cure of sandwich structures using in situ visualization

M.Anders, D.Zebrine, T.Centea, S.R.Nutt *

M.C. Gill Composites Center, Department of Chemical Engineering and Materials Science, University of Southern California, 3651 Watt Way VHE-406, Los Angeles, CA 90089-0241, USA

* E-mail: nutt@usc.edu

Abstract: Aerospace sandwich structures are often manufactured using an autoclave co-cure process, in which prepreg facesheets are cured and bonded to honeycomb core simultaneously. Co-cure involves coupled physical phenomena, including gas migration, prepreg consolidation, resin/adhesive flow and crosslinking, and potential mechanisms of defect formation. Due to the "black box" nature of the process, however, scientific understanding of the complex and interacting phenomena that cause defects remains incomplete. We address this challenge using an in situ visualization method that enables direct observation of the skin/core bond-line in realistic autoclave conditions. Five cases are presented, which span a range of process conditions leading to various defect-formation phenomena, and show the effectiveness of in-bag pressurization for preventing bond-line defects. We demonstrate that in situ diagnostics can eliminate much of the trial-and-error typically involved in process troubleshooting, by providing insights into the physics of co-cure that would otherwise be difficult to obtain.

Key words: A (Material): Sandwich structures; B (Property): Cure behaviour; D (Testing): Process monitoring; E (Manufacturing/Processing): Autoclave

1. INTRODUCTION

Composite honeycomb sandwich structures consist of two prepreg facesheets (or "skins"), bonded with a film adhesive to either side of a low-density, hexagonal-cell Nomex or aluminum core

Please cite the article as: Anders M, Zebrine D, Centea T, Nutt S. **Process diagnostics for co-cure of sandwich structures using in situ visualization**. Composites Part A. 2019; 116:24-35. **DOI**: 10.1016/j.compositesa.2018.09.029

[1]. The skins and film adhesive are often co-cured in a single process cycle under elevated temperature and pressure within an autoclave, using a one-sided tool and enveloped in a vacuum bag.

The co-cure process consists of the following steps. First, under ambient external temperature and pressure, vacuum is pulled within the vacuum bag to consolidate the prepreg plies and to remove air initially entrapped between them. After some time – which varies depending on part size and other factors – autoclave pressure is applied, further compacting the sandwich structure. Often, the vacuum bag is either brought to partial vacuum or fully vented to atmospheric pressure. Next, the temperature is increased to reduce the prepreg resin and adhesive viscosities. An isothermal dwell provides time for flow to occur, as surface tension causes the adhesive to form fillets along the edges of the cell walls against the prepreg skin [2]. Finally, a second dwell at a higher temperature causes the resin and adhesive to gel and vitrify, after which the autoclave can be cooled and depressurized, and the finished part can be removed.

Manufacturing defects associated with any of the three components – skin, adhesive, and core – can occur during processing [1]. The discontinuous honeycomb substrate can lead to compaction variations and dimpling within the skins, as well as resin bleed into the open core cells, causing skin porosity due to resin starvation. Additionally, the gas in the core cells can be driven through the prepreg – which, if it occurs during resin gelation, results in skin porosity – and low gas pressure in the core can lead to a reduction in the hydrostatic pressure of the prepreg resin, potentially allowing bubble nucleation/growth from dissolved volatile species and further contributing to porosity in the skins [3]. Adhesive fillets can also be disrupted by analogous phenomena: low pressures can lead to bubble nucleation/growth from volatile release, gas migrating through the adhesive can get locked in place during gelation, and excessive flow can cause dripping/bleeding into undesired locations.

Please cite the article as: Anders M, Zebrine D, Centea T, Nutt S. **Process diagnostics for co-cure of sandwich structures using in situ visualization**. Composites Part A. 2019; 116:24-35. **DOI**: 10.1016/j.compositesa.2018.09.029

Finally, defects relating to deformation of the honeycomb core can arise if excess autoclave pressure is applied [4], although these issues are beyond the scope of the present work.

The traditional means of quality assurance and process refinement typically rely on ex situ inspection, i.e., parts are inspected outside of the processing environment after cure. While process variables such as temperatures and pressures are measured during autoclave processing, the autoclave and vacuum bag serve as barriers that prevent real-time monitoring of microstructural changes (e.g., void formation). Fig. 1 shows polished sections of co-cured samples to emphasize the limitations of post-mortem analysis and motivate the need for in situ process diagnostics. These samples consist of the same materials and were cured under the same temperature cycle, but other process modifications (namely the initial adhesive format, the breathability of the core, and the pressure cycle) caused significant variations in part quality (a detailed description of the process parameters for these samples is given in Section 3.2). The images in Fig. 1 provide information about the final state of the parts, but supply little insight into the co-cure process. How, when, and why did these bond-lines evolve into their final states? What phenomena are responsible for causing such variability in skin and bond-line quality?

Please cite the article as: Anders M, Zebrine D, Centea T, Nutt S. **Process diagnostics for co-cure of sandwich structures using in situ visualization**. Composites Part A. 2019; 116:24-35. **DOI**: 10.1016/j.compositesa.2018.09.029

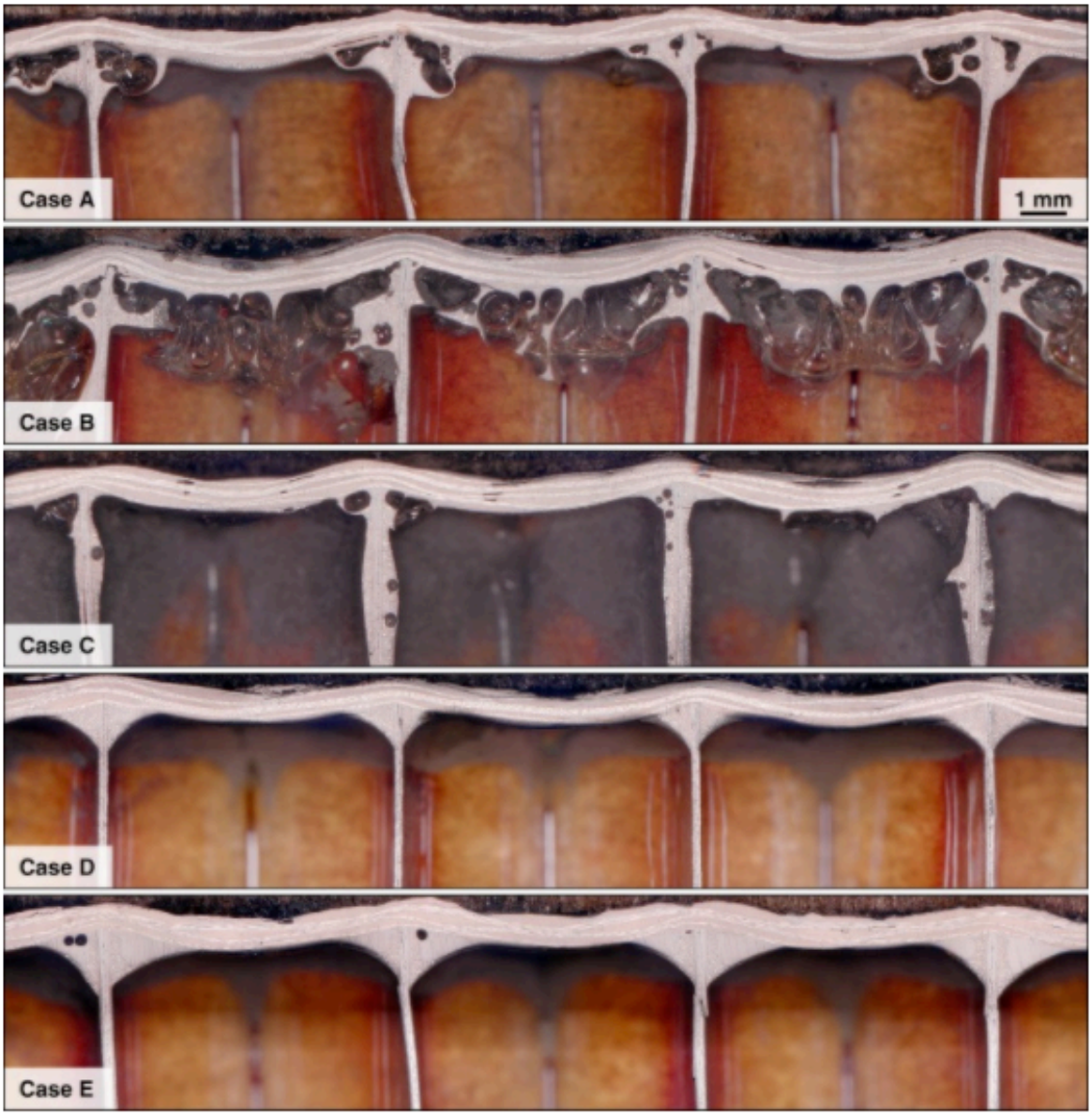

Fig. 1. Polished-section micrographs of co-cured samples exhibiting a wide range of morphologies. (For interpretation of the references to colour in this figure legend, the reader is referred to the web version of this article.)

To reliably fabricate defect-free sandwich structures, we must identify the relevant process phenomena, characterize the time-dependent material behaviors, and develop appropriate processes based on scientific understanding. To achieve these goals, we implement an experimental method

Please cite the article as: Anders M, Zebrine D, Centea T, Nutt S. **Process diagnostics for co-cure of sandwich structures using in situ visualization**. Composites Part A. 2019; 116:24-35. **DOI**: 10.1016/j.compositesa.2018.09.029

that enables in situ observations of bond-line evolution during autoclave co-cure. The work was inspired by – and builds upon – previous research described in the following section.

1.1. Literature review

While co-cure is inherently a complex process involving coupled phenomena, much of the relevant material behavior has been investigated in simpler contexts. For example, Pearce et al. [5] studied void formation in film adhesives during secondary bonding of honeycomb core to glass and metal substrates. They found volatile release at sub-ambient core pressures to be the primary cause of voids, and using FTIR spectroscopy, they identified the volatiles as water (absorbed from environmental humidity) and residual solvent (from the filming process). Hayes et al. [6] studied another simplified system: honeycomb sandwich structures without film adhesive, using "self-adhesive" prepregs for which excess prepreg resin formed the skin/core bond-line. They compared prepregs fabricated by both a solvent-based process and a hot-melt process, and found that residual solvent in the former case caused significantly higher void content in both the skins and fillets. Also using a self-adhesive prepreg/honeycomb system, Yuan et al. [7] studied the influence of process parameters (cure temperature and pressure cycle) on part quality. They measured internal core pressure by inserting a capillary tube into the honeycomb, and found that higher-rate temperature ramps increased the buildup of core pressure, as well as the final void content. They also reported that full autoclave pressure throughout processing resulted in resin bleed and skin porosity from resin starvation. However, delaying the application of autoclave pressure until just before gelation prevented these problems.

Researchers have attempted to correlate mechanical properties of cured sandwich structures (e.g., flatwise tensile strength, peel strength, lap shear strength, etc.) with material and process inputs [8], [9], [10], [11], [12], [13]. Due to the complexity of the co-cure process, however, these studies

Please cite the article as: Anders M, Zebrine D, Centea T, Nutt S. **Process diagnostics for co-cure of sandwich structures using in situ visualization**. Composites Part A. 2019; 116:24-35. **DOI**: 10.1016/j.compositesa.2018.09.029

often resort to statistical techniques such as design of experiments (DoE) and analysis of variance (ANOVA) [8]. Such approaches can be useful in identifying statistically-significant trends, but do not offer a complete understanding of the underlying physics. Thus, while they can be used to determine "optimal" process parameters for a given set of materials, they provide limited insight into why a particular set of parameters results in a particular outcome. Furthermore, the conclusions from such studies cannot necessarily be applied to other materials. Due to the coupling of various process phenomena, even seemingly minor changes to the materials or process can have far-reaching and potentially counterintuitive consequences. For example, Hou et al. [9] observed that certain adhesives foamed under vacuum at cure temperatures, while others did not, but that foaminess was not a reliable indicator of flatwise tensile strength. They showed that a thermal aging pretreatment of one adhesive increased the minimum viscosity during cure, reducing the severity of foaming and leading to an increase in flatwise tensile strength, while another adhesive with an even higher minimum viscosity did not foam at all, yet exhibited the lowest flatwise tensile strength (a different problem – poor wetting and inferior fillet formation – occurred in that case). Nagarajan et al. [10] noted similar complications in interpreting results of a DoE/ANOVA study, due to strong interactions between factors. In particular, the factor levels that resulted in higher mechanical properties for samples with standard aluminum honeycomb generally had the opposite effect for samples with a "vented" core structure. Overall, samples with larger fillets and fewer voids had superior properties, but how and why a given set of process parameters led to a specific bond-line morphology remained unclear.

A recurring theme in the literature on sandwich panel manufacturing is the importance of the gas pressure within the core cells: it directly affects the hydrostatic pressure of the resin/adhesive at the skin/core interface, and is thus a key parameter influencing void formation. The core pressure is

Please cite the article as: Anders M, Zebrine D, Centea T, Nutt S. **Process diagnostics for co-cure of sandwich structures using in situ visualization**. Composites Part A. 2019; 116:24-35. **DOI**: 10.1016/j.compositesa.2018.09.029

influenced by multiple competing factors, making it difficult to predict, and measuring core pressure in a real sandwich panel during autoclave cure is highly impractical. Two bodies of work – those of Tavares et al. [14], [15], [16], [17], [18] and Kratz & Hubert [19], [20], [21], [22] – address these challenges and describe the behavior of core pressure in the context of vacuum bag-only (VBO) co-cure (i.e., using only atmospheric pressure, instead of elevated autoclave pressure, to provide compaction). Both groups utilized lab-scale experimental fixtures, which consisted of tool plates containing recessed pockets. Honeycomb core was placed into the pocket and covered with prepreg, forming a "half-sandwich" assembly, and a gas pressure sensor connected to the interior of the now-sealed pocket was used to measure the simulated "core" pressure.

Tavares et al. described a falling-pressure method to characterize the air permeability K of prepreg skins, and showed a dependence on resin viscosity [14]. They considered the influences of the film adhesive and the initial impregnation state of the prepreg on both gas migration through the skin, and on resin bleeding into the core cells [15]. They also explored the effects of skin modifications (perforations in each ply, perforations through the entire skin, etc.) on air permeability [16]. The various skin-modification schemes resulted in varying ranges of core pressures, and the authors noted that different issues arose at opposite extremes of core pressure: low core pressures caused volatile-induced void formation within the adhesive, while high core pressures resulted in small fillets due to insufficient compressive force between the skin and core. An intermediate core pressure range of 40–70 kPa limited the severity of both of these issues and resulted in samples with the greatest peel fracture energy [17].

Using a similar experimental setup for single-skinned "half-sandwich" assemblies, Kratz & Hubert also measured core pressure during room-temperature vacuum holds and during cure [19]. Unidirectional fabrics were effectively impermeable over a 24-hour vacuum hold [20], because the

Please cite the article as: Anders M, Zebrine D, Centea T, Nutt S. **Process diagnostics for co-cure of sandwich structures using in situ visualization**. Composites Part A. 2019; 116:24-35. **DOI**: 10.1016/j.compositesa.2018.09.029

pressure difference across the skin was insufficient to overcome the capillary pressure of the viscous resin between the closely-spaced fibers. Conversely, woven fabrics allowed through-thickness air evacuation because the fabric structure included larger macro-pores between the overlapping fiber tows (where gas must overcome a lower capillary pressure to displace liquid resin). However, a delay was observed between the application of vacuum and the onset of core evacuation, attributed to the transient process of air displacing resin to form continuous open channels through the skin. Also, the evacuation process halted before the core pressure fell to match the vacuum bag pressure, resulting in a residual core pressure. At this point, the gas pressure in the air channels became insufficient to balance the surrounding resin pressure, causing the channels to close and preventing further gas flow through the skin.

During cure, the core pressure depended on competing factors [21]. Continual evacuation through the skin – governed by the prepreg air permeability – tended to reduce the core pressure, while pressure increased upon heating due to ideal gas law behavior and the vaporization of moisture (initially absorbed by the organic Nomex honeycomb core from ambient humidity). Based on these phenomena, a model for core pressure was developed and compared to measured core pressures in full-scale sandwich structures using embedded MEMS sensors [22]. The model/experiment comparisons affirmed the validity of the assumption that a single-skinned co-cured structure could be used to characterize the processing of realistic sandwich structures.

For all of the aforementioned studies, visual inspection of sandwich structures was limited to ex situ methods (e.g., optical microscopy of polished sections and computed X-ray tomography [19], [20], [23]), which cannot adequately characterize the transient process phenomena that occur during co-cure. We have published preliminary results for an in situ visualization concept: a simplified method [24] using a windowed tool that was originally designed for resin transfer molding [25], and

Please cite the article as: Anders M, Zebrine D, Centea T, Nutt S. **Process diagnostics for co-cure of sandwich structures using in situ visualization**. Composites Part A. 2019; 116:24-35. **DOI**: 10.1016/j.compositesa.2018.09.029

initial exploratory tests [26], [27] using the tool described here. This article expands on the previous work by presenting an application of the in situ diagnostic method: first, the causes of observed bond-line defects are identified and explained, and subsequently, a solution strategy is proposed and demonstrated to be effective at preventing bond-line defects.

1.2. Objective & approach

The objectives of this work are (1) to reveal the dynamic behavior of bond-line evolution and the aforementioned defect formation phenomena during co-cure in realistic autoclave conditions, and (2) to demonstrate the utility of in situ visualization as a diagnostic tool for the co-cure process. We present a case study consisting of five co-cure experiments. The test parameters were selected to showcase a variety of process conditions and phenomena, and to exemplify insight-driven process design. In lieu of using a DoE approach to correlate process parameters with manufacturing defects, we identified sources of defects through direct visual observations, and implemented informed process modifications to prevent the observed defect formation mechanisms. The order in which the cases are presented follows a logical narrative: each of the first three cases (A, B, & C) exhibited a distinct type of defect formation, which was addressed by modifying the subsequent case. After three iterations of identifying and addressing process-induced defect mechanisms, the fourth experiment (Case D) resulted in an "ideal" sample. Finally, Case E tested the feasibility of utilizing the strategy from Case D (which included an "equilibrated core" condition) in the most generic case of co-cure (i.e., where the core pressure can differ from the vacuum bag pressure).

Please cite the article as: Anders M, Zebrine D, Centea T, Nutt S. **Process diagnostics for co-cure of sandwich structures using in situ visualization**. Composites Part A. 2019; 116:24-35. **DOI**: 10.1016/j.compositesa.2018.09.029

2. EXPERIMENTAL FACILITIES

The design of our system is based on the concept used by Tavares and Kratz, but augmented with additional capabilities. Fig. 2 shows a CAD rendering of the tool, sectioned at the mid-plane to reveal interior features. The main lower component is a 280 mm square anodized aluminum plate containing a centrally-located 76 mm square pocket (19 mm depth). A 12.7 mm thick glass disk with conically-tapered sides is mounted in a matching hole at the center of the tool plate pocket, with silicone sealant at the tapered interface providing an airtight seal. Square glass spacers of varying thickness can be placed into the pocket, to accommodate varying thicknesses of honeycomb core that are placed above, such that the top of the honeycomb is flush with the plane of the tool plate. A prepreg skin is shown extending beyond the edges of the pocket to form an “edge band” that seals the interior of the core pocket. Consumables (edge dams, release film, and breather cloth) surround the sample, and a vacuum bag film is located above, sealed around the perimeter with tacky-tape. A hole near the corner of the tool plate (not visible in Fig. 2) is located under the breather cloth inside the sealed perimeter of the vacuum bag, enabling the application of vacuum within the bagging assembly through a port on the underside of the tool plate. Another port (the “core vent”) is located in a corner of the core pocket, allowing the gas pressure in the core cavity to be controlled, if desired. A self-sealing fitting prevents gas flow through this port when not in use.

Please cite the article as: Anders M, Zebrine D, Centea T, Nutt S. **Process diagnostics for co-cure of sandwich structures using in situ visualization**. Composites Part A. 2019; 116:24-35. **DOI**: 10.1016/j.compositesa.2018.09.029

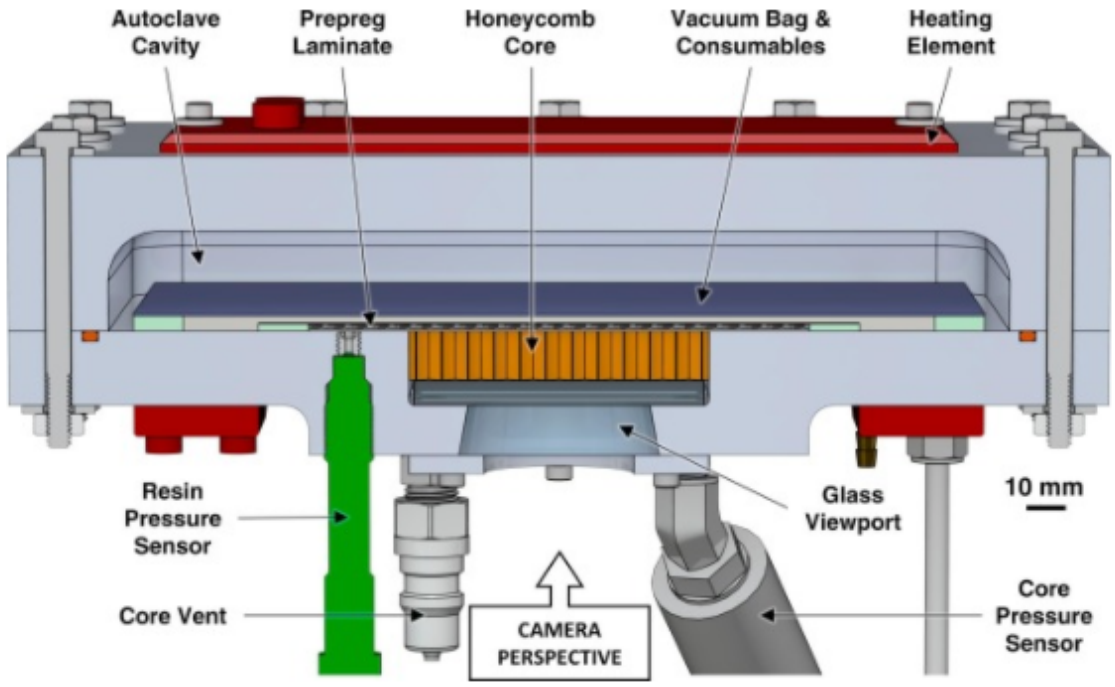

Fig. 2. Section view of co-cure fixture with sample and consumables. (For interpretation of the references to colour in this figure legend, the reader is referred to the web version of this article.)

The upper large component shown in Fig. 2 is an aluminum block with a hollowed-out underside that is bolted onto the tool plate through a set of holes around the perimeter. An O-ring groove at the interface between the lower and upper aluminum parts (the tool plate and the "lid") creates a sealed environment, and a port through the tool plate (located outside the perimeter of the vacuum bag) allows the internal "autoclave cavity" to be pressurized. Traditionally, the molding tool for an autoclaved part is a stand-alone structure that can be moved in and out of the autoclave. In this case, however, the lower aluminum piece acts as both a tool plate and as part of the "autoclave" pressure vessel. This design enables the observation of the interior of a co-cured part from outside the autoclave.

The tool plate contains a pass-through for thermocouple wires to measure temperature at desired locations in and around the vacuum bag assembly. The upper and lower aluminum blocks contain

Please cite the article as: Anders M, Zebrine D, Centea T, Nutt S. **Process diagnostics for co-cure of sandwich structures using in situ visualization**. Composites Part A. 2019; 116:24-35. **DOI**: 10.1016/j.compositesa.2018.09.029

resistive heating elements, which can be controlled independently through a pair of PID controllers (Watlow model PM6R1CA). The system was designed to safely support temperatures up to 200 °C and autoclave pressures up to 800 kPa.

Pressure transducers (Omega model PX32B1) measure gas pressure in the hoses providing vacuum and autoclave pressures (P_{bag} and P_{auto}, respectively). A port in the corner of the core cavity pocket connects to another transducer that measures the gas pressure within the core (P_{core}). The interface between the glass spacer and the honeycomb core is intentionally not airtight, allowing gas pressure to equalize everywhere within the core cavity (i.e., the pressure in the core cells visible through the window equals the pressure measured by the core pressure transducer). A fourth pressure transducer (Gefran ME2 series), mounted in the tool plate, measures the prepreg resin pressure in the edge band. However, the design of this feature renders the measurements susceptible to artefacts that complicate interpretation. The data from this transducer does not contribute meaningfully to the results of this study, and is thus omitted from subsequent discussion to avoid potential confusion.

The tool plate and lid assembly is mounted on a frame (shown in Fig. 3), allowing a portable digital microscope (Dino-Lite Edge AM7815MZTL) to be located under the tool, facing upwards at the window. The frame also contains an enclosure that houses the power supplies for the heaters and sensors.

Please cite the article as: Anders M, Zebrine D, Centea T, Nutt S. **Process diagnostics for co-cure of sandwich structures using in situ visualization**. Composites Part A. 2019; 116:24-35. **DOI**: 10.1016/j.compositesa.2018.09.029

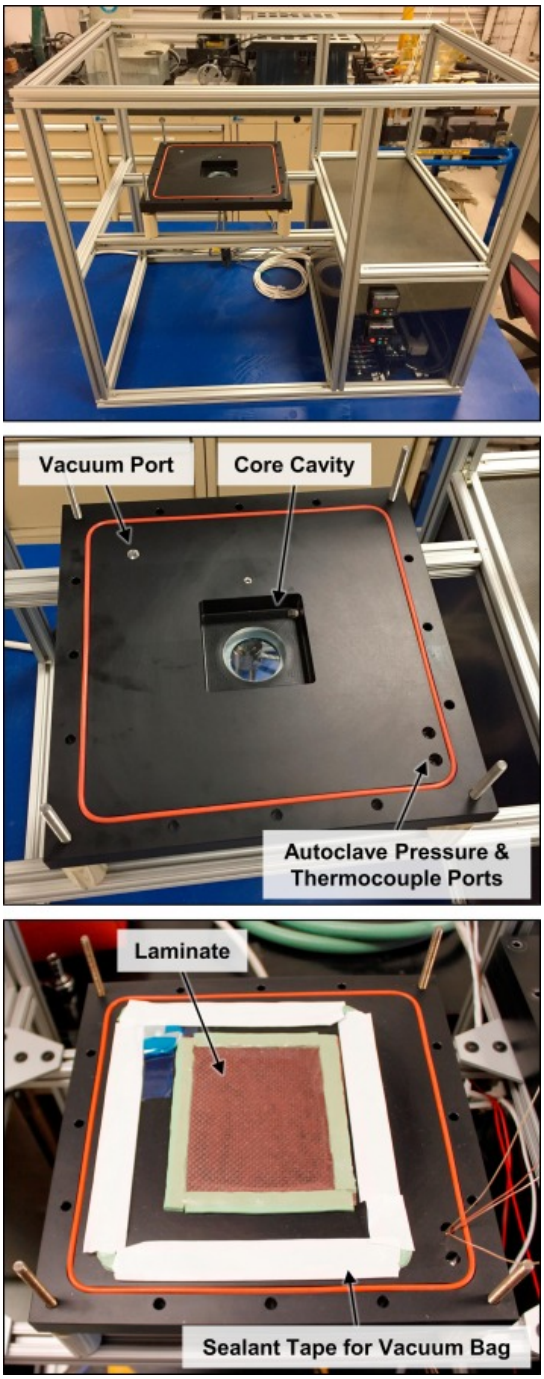

Fig. 3. Photographs of the co-cure fixture. Top: frame with lower half of tool (left) and power-distribution enclosure (right). Middle: close-up of tool plate. Bottom: tool plate with laminate. (For interpretation of the references to colour in this figure legend, the reader is referred to the web version of this article.)

Autoclave pressure is supplied by an air compressor and controlled using a regulator and overpressure relief valve. A vacuum pump connects to the vacuum bag port, and for tests with an

Please cite the article as: Anders M, Zebrine D, Centea T, Nutt S. **Process diagnostics for co-cure of sandwich structures using in situ visualization**. Composites Part A. 2019; 116:24-35. **DOI**: 10.1016/j.compositesa.2018.09.029

"equilibrated core" condition (explained in Section 3.2), another hose from the (otherwise sealed) core vent is connected to the main vacuum line using a T-junction. Furthermore, using a three-way valve, the vacuum line can be switched such that a compressed nitrogen tank, rather than the vacuum pump, is connected to the vacuum bag. This configuration enables venting of the bag using dry N2 (versus potentially humid air from the environment), but more importantly, it allows super-ambient pressures to be applied within the vacuum bag. This "in-bag pressurization" concept is explained in greater detail in Section 3.2.

Temperature and pressure signals are acquired using a digital data acquisition system (cDAQ-9174, National Instruments) and recorded using a LabVIEW interface on a desktop PC. The same PC receives images from the digital microscope, and timestamps on both types of data enable synchronization.

Prior to sample fabrication, all pressure transducers were calibrated over the relevant range of process pressures and temperatures. Errors in reported pressure values due to thermal drift were < 3 kPa. Leak testing of the core cavity was performed by sealing a metal plate over the core pocket, evacuating the core cavity using the core vent, and monitoring changes in core pressure after removal of the vacuum hose. Threads on the fittings (which included a slow-curing liquid thread sealant) were tightened until, at both room temperature and the maximum process temperature, no detectable changes in core pressure occurred over a minimum duration of 1 h.

3. EXPERIMENTAL METHODS

3.1. Materials and layup

The prepreg skins consisted of a widely-used carbon/epoxy autoclave prepreg (HexPly AGP193PW/8552S, Hexcel Corp., AS4 fibers, 193 g/m2 fiber areal weight, 3000 fibers/tow, plain

Please cite the article as: Anders M, Zebrine D, Centea T, Nutt S. **Process diagnostics for co-cure of sandwich structures using in situ visualization**. Composites Part A. 2019; 116:24-35. **DOI**: 10.1016/j.compositesa.2018.09.029

weave fabric, fully-saturated with 38% by weight 8552 toughened epoxy resin). The trailing "S" indicates the prepreg was manufactured by a solvated tower process [28].

The adhesive was a toughened epoxy film (Loctite EA 9658 AERO 060UNS, Henkel Corp.) with 290 g/m2 areal weight and no supporting carrier, designed for metal, composite, and honeycomb bonding in aircraft engine nacelles [29]. The viscosity of this adhesive is tailored for "controlled flow" [30], to prevent issues such as hole blockage from excessive bleed, and to provide a "reticulation" capability. Although many film adhesives are supported by a lightweight carrier film (typically nonwoven glass or polymer fibers), EA 9658 AERO is offered in the unsupported "UNS" form so that it can be placed onto honeycomb core and then reticulated. The reticulation process – which can be performed in several ways [11], [31] – results in adhesive located only along the edges of the honeycomb cell walls, with an opening in the film at the center of each cell. Fig. 4 shows the stages of adhesive reticulation. First, the adhesive film was placed onto the top side of the honeycomb core and manually perforated in the center of each honeycomb cell using a ~1 mm diameter needle. Then, heated air was blown over the surface of the film using a handheld hot-air gun. As the film softened under the applied heat, surface tension caused the holes to widen, reshaping the film into an adhesive bead along the edges of the cell walls. Temperatures were monitored using a thermocouple and did not exceed 70 °C. Reticulation was completed in < 3 min, ensuring that the process did not advance the cure of the adhesive.

Please cite the article as: Anders M, Zebrine D, Centea T, Nutt S. **Process diagnostics for co-cure of sandwich structures using in situ visualization**. Composites Part A. 2019; 116:24-35. **DOI**: 10.1016/j.compositesa.2018.09.029

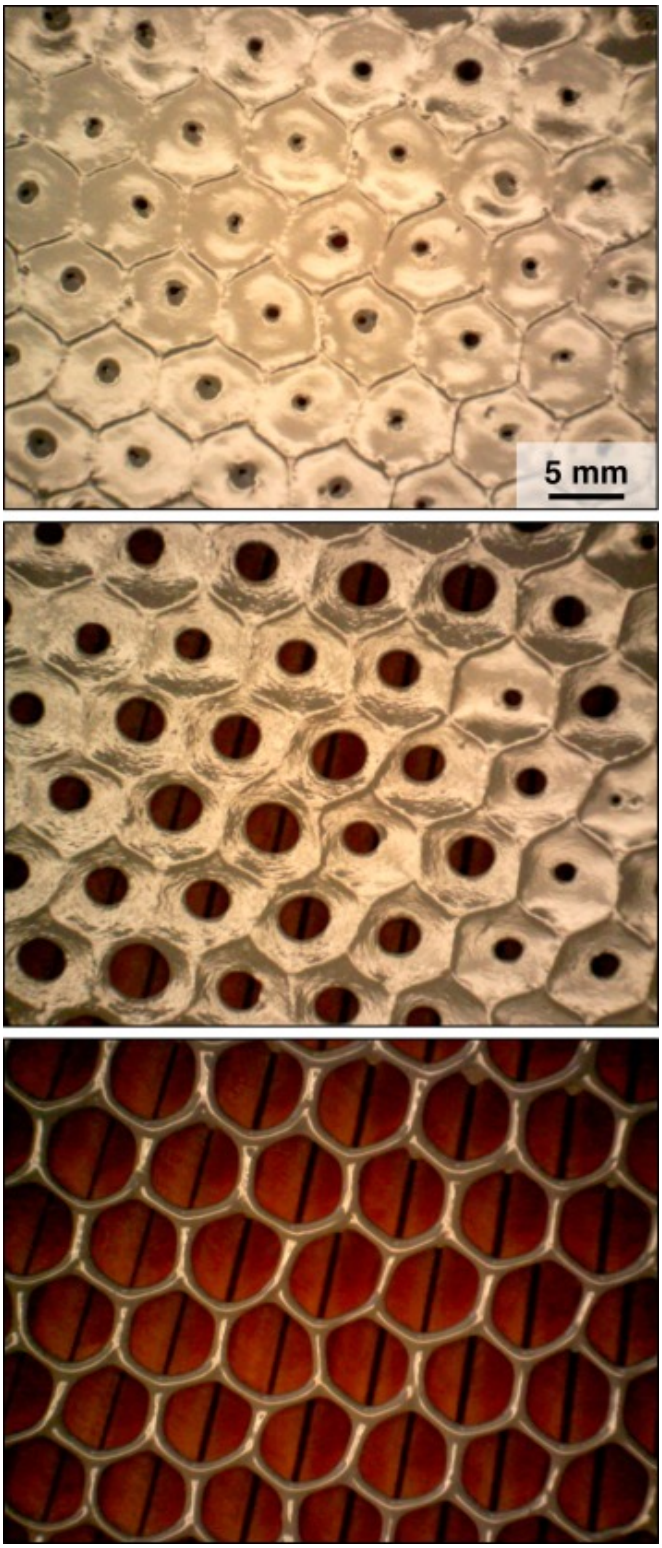

Fig. 4. Stages of the adhesive reticulation process. Top: film applied to honeycomb core and perforated. Middle: film softening under applied heat and perforations opening due to surface tension. Bottom: process completed when adhesive forms a bead along the edges of the cell walls. (For interpretation of the references to colour in this figure legend, the reader is referred to the web version of this article.)

Please cite the article as: Anders M, Zebrine D, Centea T, Nutt S. **Process diagnostics for co-cure of sandwich structures using in situ visualization**. Composites Part A. 2019; 116:24-35. **DOI**: 10.1016/j.compositesa.2018.09.029


The honeycomb core consisted of a phenolic-coated aramid (Nomex) paper (Gillcore HD433, The Gill Corp., 6.4 mm cell diameter, 12.7 mm thickness, 48 kg/m3 density).

Identical material kits (consisting of core, one adhesive layer, four prepreg plies, and vacuum bag consumables) were used for all samples. First, a liquid mold-release agent (Frekote 770-NC, Henkel Corp.) was applied to the tool surfaces and to a glass spacer in the bottom of the core pocket. A 76 mm square of honeycomb core was placed into the pocket, its top surface flush with the plane of the tool plate. Four plies of prepreg were cut into 126 mm squares, providing a 25 mm edge band to extend beyond the edges of the core pocket. The plies were stacked in a (0°)2S orientation, one layer of film adhesive (also 126 mm square) was applied to the underside, and the completed skin was placed onto the tool, centered over the core pocket. In cases where the adhesive was reticulated, a 76 mm square was cut from the center of the 126 mm square of adhesive film and applied onto the core (as described above) prior to placing it into the core pocket. The remaining “frame” of film adhesive was applied to the prepreg skin, so in all cases the edge band contained a continuous adhesive layer between the tool plate and the first prepreg ply. The primary reason for extending the film adhesive beyond the edges of the core and into the edge band was to ensure that no leak path existed between the core cavity and the vacuum bag. If the textured surface of the prepreg were directly against the tool plate, gas pathways could exist at the interface. Conversely, the smooth surface of the film adhesive against the tool plate reliably formed an airtight seal.

The prepreg edges were sealed with tacky tape (GS 213, Airtech Intl.) to enforce out-of-plane gas transport only. This configuration approximates the center of a large sandwich structure, far from any breathing edges. A perforated release film (A4000, Airtech Intl.) was placed over the prepreg skin, then a breather cloth (Airweave N10, Airtech Intl.), and finally a vacuum bag film (Wrightlon

Please cite the article as: Anders M, Zebrine D, Centea T, Nutt S. **Process diagnostics for co-cure of sandwich structures using in situ visualization**. Composites Part A. 2019; 116:24-35. **DOI**: 10.1016/j.compositesa.2018.09.029

7400, Airtech Intl.) was placed over the entire assembly and sealed to the edges of the tool plate with tacky tape.

3.2. Process parameters for case study

The thermal cycle used for all cases is shown in Fig. 5, and closely resembles the manufacturer-recommended cure cycle for the prepreg [28]. After a one-hour room-temperature dwell, the temperature was raised to 110 °C and held for one hour, then raised to 177 °C and held for two hours (all temperature ramps were 2 °C/minute). The room-temperature, intermediate-temperature, and high-temperature stages will be referred to as Stages I, II, and III, respectively.

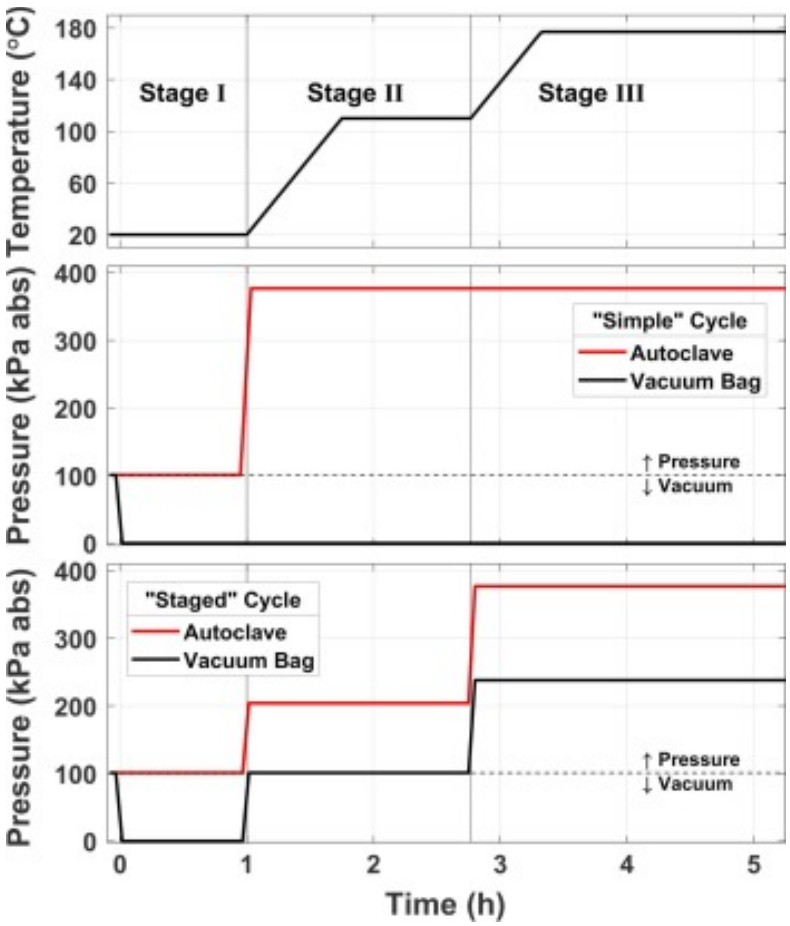

Fig. 5. The temperature cycle used for all tests (top), and the two cycles used for autoclave and vacuum bag pressures (middle and bottom). Stages I, II, and III denote room-temperature, intermediate-temperature, and high-temperature stages (respectively) of the process. (For interpretation of the references to colour in this figure legend, the reader is referred to the web version of this article.)

Please cite the article as: Anders M, Zebrine D, Centea T, Nutt S. **Process diagnostics for co-cure of sandwich structures using in situ visualization**. Composites Part A. 2019; 116:24-35. **DOI**: 10.1016/j.compositesa.2018.09.029

Three parameters were varied between cases: the initial adhesive format, the breathability of the core, and the imposed P_{auto} and P_{bag} pressure cycles. The five test cases are represented as a "cube diagram" in Fig. 6. Each of the three axes corresponds to one of the varied parameters as described below.

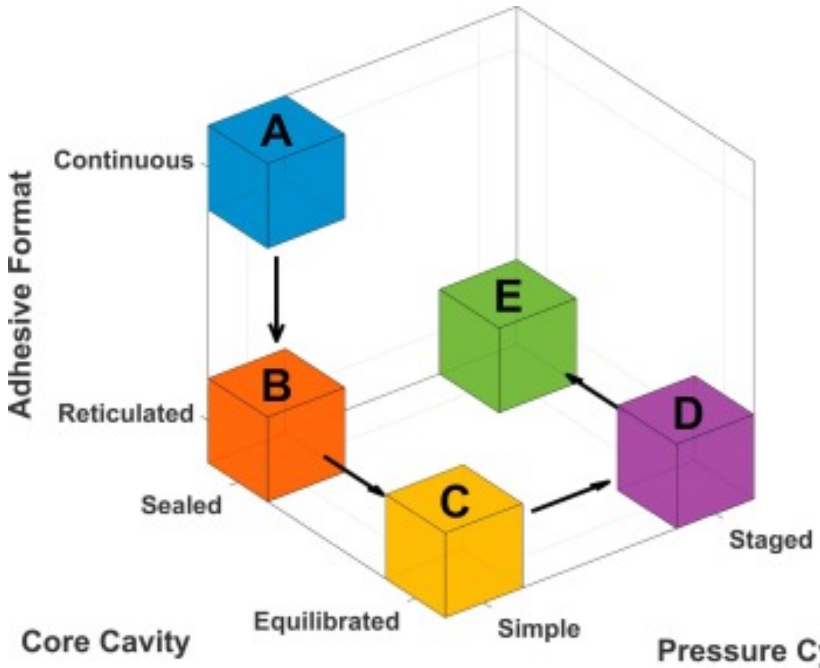

Fig. 6. Diagram of Cases A through E. The three axes denote the test variables: (1) the adhesive was either applied as a continuous film, or reticulated onto the honeycomb core; (2) the core cavity was either sealed, or connected via the "core vent" to equilibrate the gas pressure in the core cavity with that of the vacuum bag; and (3) autoclave and vacuum bag pressures were applied according to either of two cycles – "simple" or "staged" – as shown in Fig. 5. (For interpretation of the references to colour in this figure legend, the reader is referred to the web version of this article.)

3.2.1. Adhesive format

A continuous layer of film adhesive was used for Case A, while for Cases B – E, the portion of the film over the honeycomb core was reticulated (see Section 3.1 for a detailed description of the reticulation process).

Please cite the article as: Anders M, Zebrine D, Centea T, Nutt S. **Process diagnostics for co-cure of sandwich structures using in situ visualization**. Composites Part A. 2019; 116:24-35. **DOI**: 10.1016/j.compositesa.2018.09.029

3.2.2. Core breathability

Depending on the configuration of a given sandwich structure, the "breathability" of a honeycomb core insert can vary from being completely sealed to being completely equilibrated with the external environment. If the core cell walls are impermeable to gas (e.g., aluminum honeycomb), then gas transport can only occur through the skins, and the relationship between P_{core} and P_{bag} depends on the skin permeability.

Some sandwich structures, however, have a "vented" construction that allows the internal core pressure to equilibrate with external gas pressure. This can be achieved by using a honeycomb with perforations/openings in the cell walls, and by including some pathway for gas to travel between the interior and exterior of the sandwich (e.g., panels designed for acoustic damping can be fabricated using a pre-cured tool-side skin that contains pre-drilled holes [32]). In addition to acoustic applications, vented sandwich structures are commonly used to prevent moisture accumulation during service, and to relieve internal pressure buildup for space launch vehicles [33]. During processing of vented structures, P_{core} is equal to $P_{bag,}$ and can thus be directly controlled. Furthermore, because a core/bag pressure difference cannot develop, equilibrated cores avoid the possibility of driving gasses through the skin.

Cases A, B, and E were fabricated using a sealed core cavity, whereas Cases C and D simulated a vented structure with an equilibrated core, by connecting the core vent to the vacuum bag line.

3.2.3. Pressure cycle

The two pressure cycles used – "simple" and "staged" – are shown in Fig. 5. Cases A, B, and C used the simple cycle while Cases D and E used the staged cycle. The simple pressure cycle included a one-hour room-temperature vacuum hold (P_{bag}) with ambient pressure in the autoclave cavity (P_{auto}) for Stage I. Then P_{auto} was increased to 377 kPa (40 psig), and both P_{bag} and P_{auto} were held

Please cite the article as: Anders M, Zebrine D, Centea T, Nutt S. **Process diagnostics for co-cure of sandwich structures using in situ visualization**. Composites Part A. 2019; 116:24-35. **DOI**: 10.1016/j.compositesa.2018.09.029

constant during the heated portion of the cure cycle (Stages II and III). During typical autoclave processing, the vacuum bag is vented after autoclave pressure is applied, whereas for VBO processing, the bag is generally left under full vacuum throughout cure (because venting the bag would eliminate the only source of compaction pressure). The "simple" pressure cycle used here is thus atypical of autoclave cure, but showcases particular defect formation phenomena.

The staged pressure cycle was identical to the simple cycle during Stage I. However, before ramping upwards in temperature, P_{auto} was increased to 205 kPa (15 psig) and then the vacuum bag was vented with atmospheric pressure N2. These pressures were maintained until the end of Stage II, at which time P_{auto} was increased to 377 kPa (40 psig) and P_{bag} was increased to 239 kPa (20 psig).

The concept of imposing super-ambient bag and core pressures during sandwich structure manufacturing has been previously considered in the context of preventing core crush. Alteneder et al. [34] pressurized the bag and core prior to heating, and then sealed the bag such that ideal gas law behavior would further increase the pressure upon heating. This approach proved effective at preventing core crush under autoclave pressures, but the authors did not discuss the effect of in-bag pressurization on bond-line defects.

In-bag pressurization has been used to suppress void formation in monolithic laminates. This technique was developed for the Air Force in the early 1980s [35] and summarized by Campbell et al. [3]. When curing laminates with high-bleed prepregs (as opposed to low-bleed "net resin content" prepregs) by traditional autoclave methods, they measured resin pressures that initially matched the applied autoclave pressure. However, as resin bled out of the laminate, progressively more of the autoclave pressure was carried by the fiber bed and the resin pressure dropped, leading to void formation. Conversely, applying positive pressure within the bag limited the extent to which the resin pressure could drop and resulted in void-free parts. Noting the similarities between autoclave

Please cite the article as: Anders M, Zebrine D, Centea T, Nutt S. **Process diagnostics for co-cure of sandwich structures using in situ visualization**. Composites Part A. 2019; 116:24-35. **DOI**: 10.1016/j.compositesa.2018.09.029

cure of high-bleed monolithic laminates and the co-cure of sandwich structures (in which the resin pressure can drop – even in the absence of bleeding – due to low gas pressure in the core), we implemented the in-bag pressurization concept in the staged pressure cycle. Further discussion of the rationale behind the staged cycle is provided in Section 4.4.

4. RESULTS

Measured data for Cases A, B and C is shown in Fig. 7, and in situ images from these tests are shown in Fig. 8. For Cases D and E, measured data and corresponding in situ images are shown in Fig. 9 and Fig. 10, respectively. To fully appreciate the dynamic behavior captured in the visual data, the reader is strongly encouraged to view the time-lapse videos (in the supplemental materials) from which the images in Fig. 8, Fig. 10 were taken.

Please cite the article as: Anders M, Zebrine D, Centea T, Nutt S. **Process diagnostics for co-cure of sandwich structures using in situ visualization**. Composites Part A. 2019; 116:24-35. **DOI**: 10.1016/j.compositesa.2018.09.029

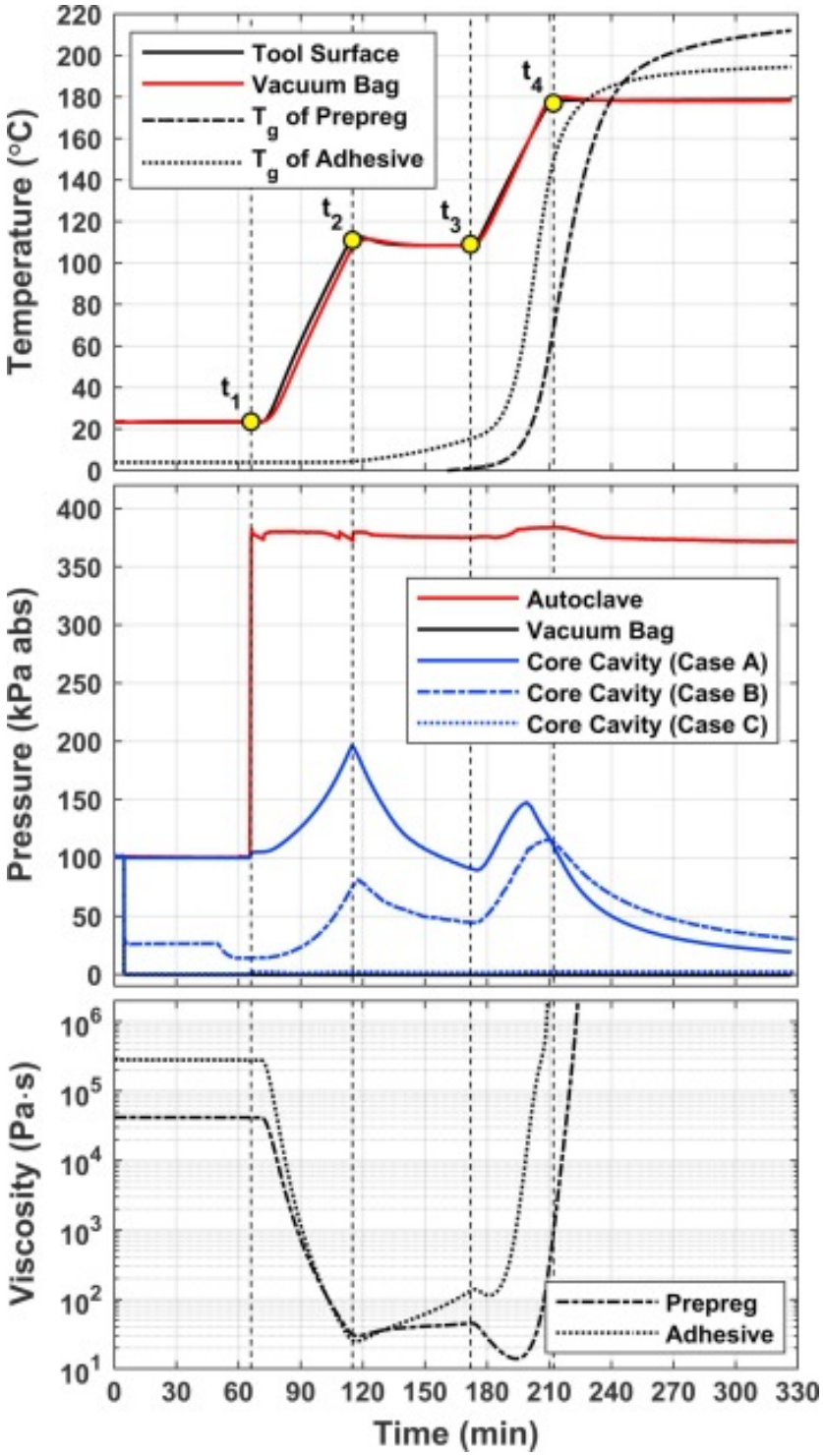

Fig. 7. Temperature and pressure data for the three cases using the "simple" pressure cycle (A, B, and C). Models for the glass transition temperature and viscosity (of both the prepreg resin and adhesive) are shown, computed from the temperature history recorded at the outside of the vacuum bag near the center of the laminate. (For interpretation of the references to colour in this figure legend, the reader is referred to the web version of this article.)

Please cite the article as: Anders M, Zebrine D, Centea T, Nutt S. **Process diagnostics for co-cure of sandwich structures using in situ visualization**. Composites Part A. 2019; 116:24-35. **DOI**: 10.1016/j.compositesa.2018.09.029

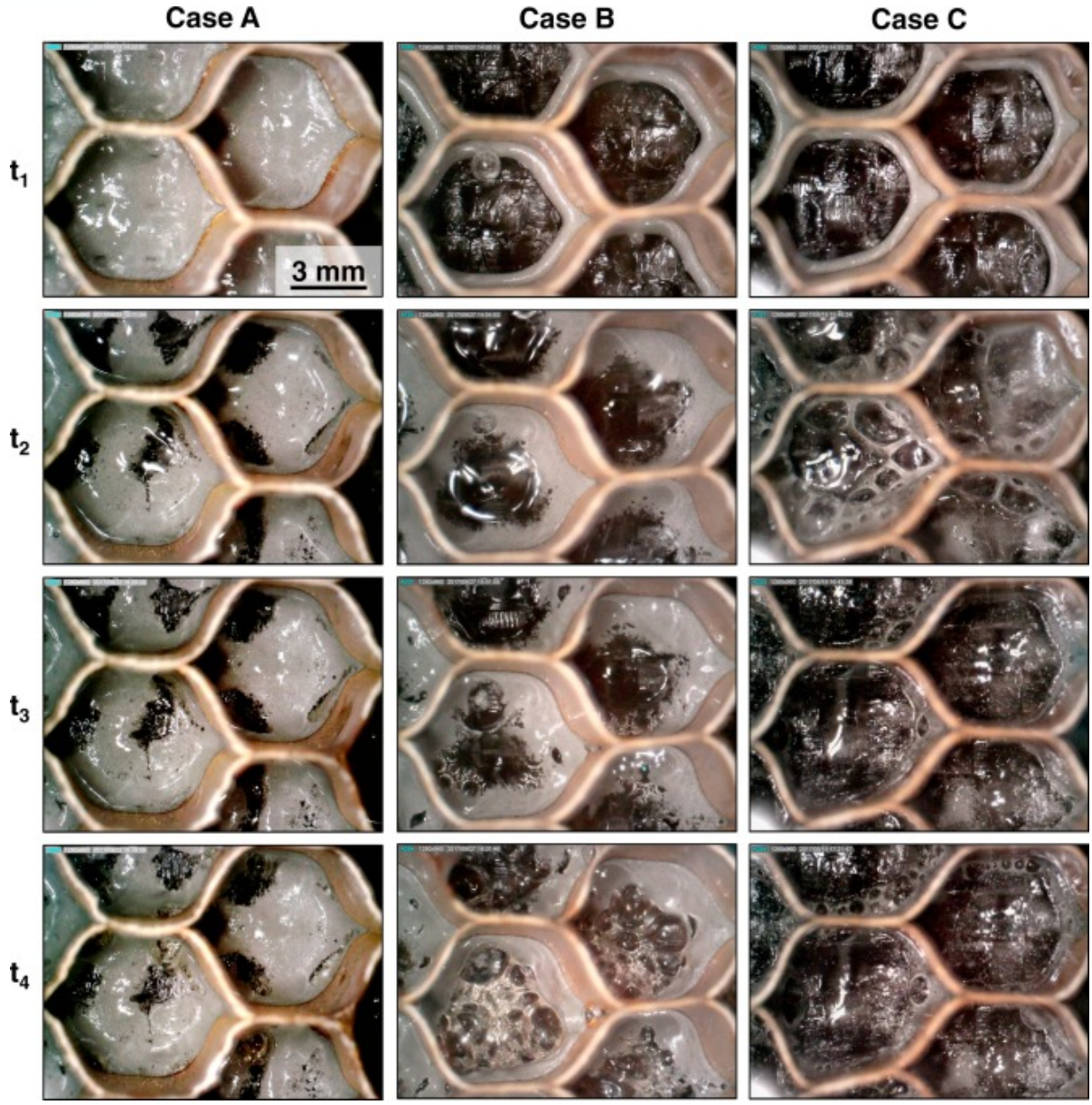

Fig. 8. In situ images of the bond-line during processing. Columns correspond to Cases A, B, and C (left to right), and rows (top to bottom) correspond to the times of interest t1 through t4 indicated on Fig. 7. (For interpretation of the references to colour in this figure legend, the reader is referred to the web version of this article.)

Please cite the article as: Anders M, Zebrine D, Centea T, Nutt S. **Process diagnostics for co-cure of sandwich structures using in situ visualization**. Composites Part A. 2019; 116:24-35. **DOI**: 10.1016/j.compositesa.2018.09.029

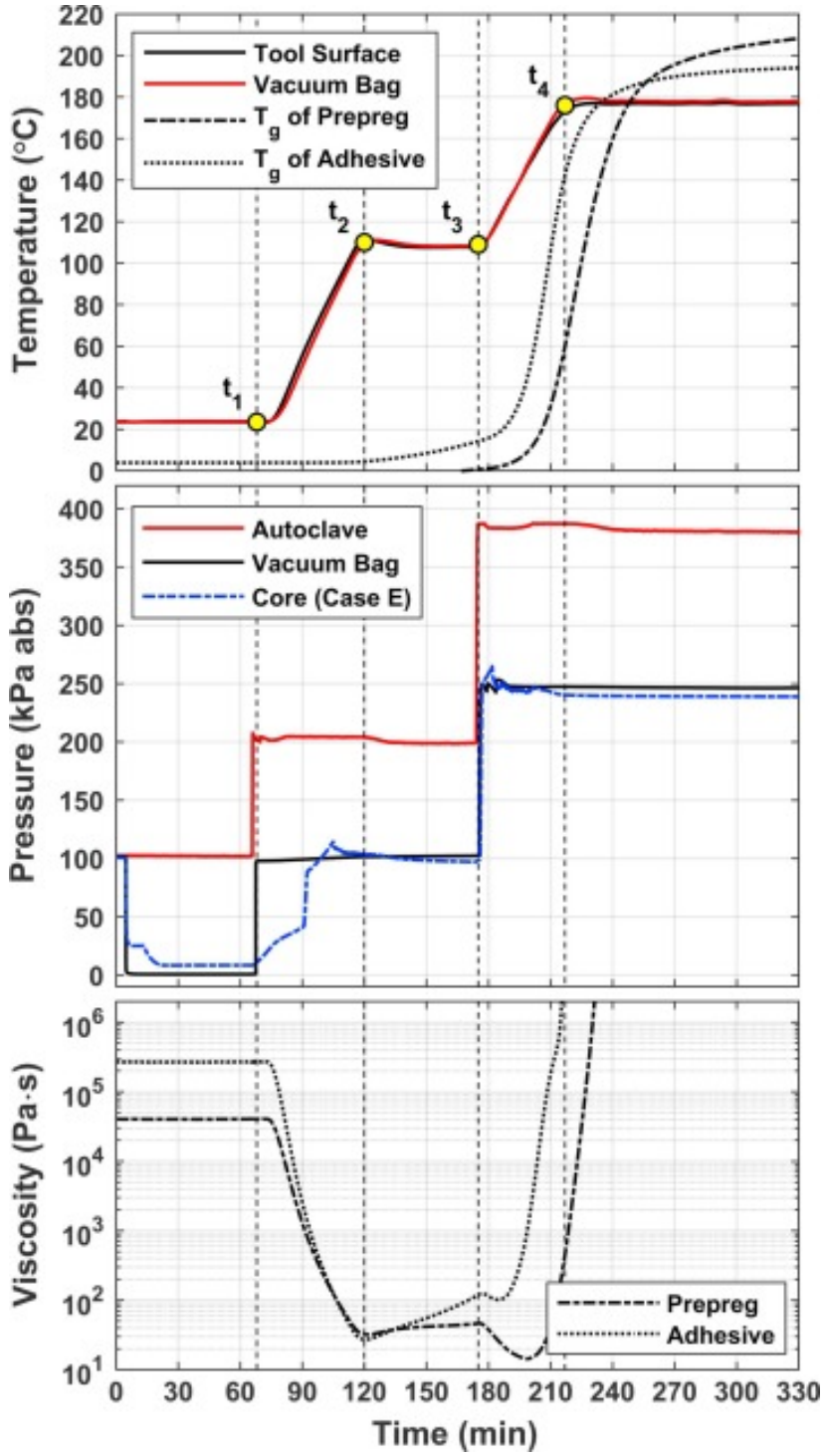

Fig. 9. Temperature and pressure data for the two cases using the "staged" pressure cycle (D and E). Models for the glass transition temperature and viscosity (of both the prepreg resin and adhesive) are shown, computed from the temperature history recorded at the outside of the vacuum bag near the center of the laminate. (For interpretation of the references to colour in this figure legend, the reader is referred to the web version of this article.)

Please cite the article as: Anders M, Zebrine D, Centea T, Nutt S. **Process diagnostics for co-cure of sandwich structures using in situ visualization**. Composites Part A. 2019; 116:24-35. **DOI**: 10.1016/j.compositesa.2018.09.029

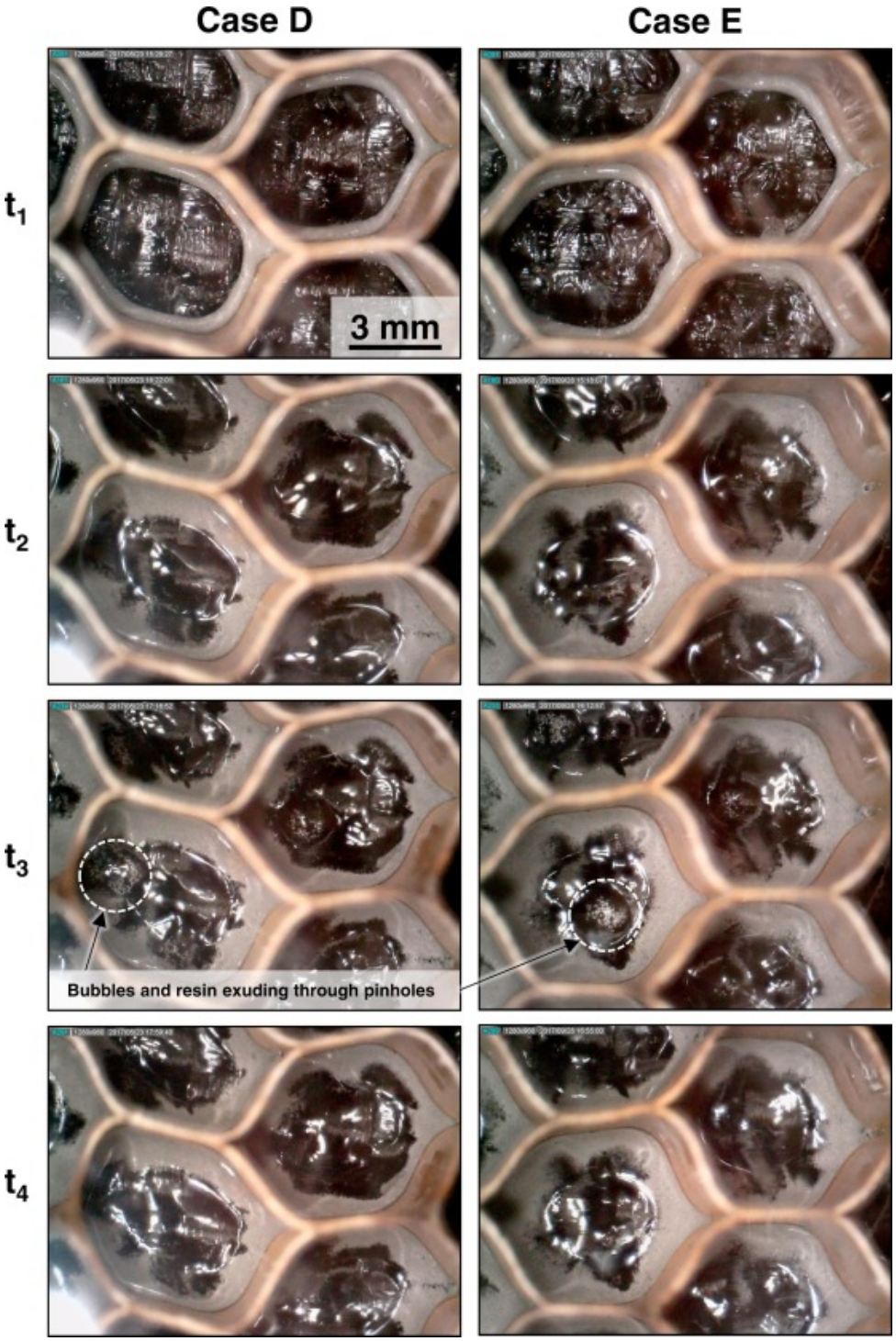

Fig. 10. In situ *images of the bond-line during processing. Columns correspond to Cases D and E (left to right), and rows (top to bottom) correspond to the times of interest* t1 *through* t4 *indicated on Fig. 9. (For interpretation of the references to colour in this figure legend, the reader is referred to the web version of this article.)*

Please cite the article as: Anders M, Zebrine D, Centea T, Nutt S. **Process diagnostics for co-cure of sandwich structures using in situ visualization**. Composites Part A. 2019; 116:24-35. **DOI**: 10.1016/j.compositesa.2018.09.029

4.1. Case A

Fig. 7 shows the measured temperatures (top) and pressures (middle) for Case A, which featured a continuous adhesive film, a sealed core, and the simple pressure cycle. Previously developed models [24], [36] were used to compute the glass transition temperature Tg of the prepreg and adhesive, as well as the viscosity profiles (bottom graph). The indicated times of interest t1 through t4 correspond to the images in the left column of Fig. 8.

Upon application of vacuum within the bag, P_{core} remained unchanged, since the continuous adhesive film acted as a barrier for gas transport. Little change was observed visually during Stage I, although significant flow occurred as the temperature was raised between t1 and t2. First, prepreg resin (which is clear, while the aluminum-powder-filled adhesive is gray) pushed through the adhesive film in a grid-like pattern, clearly emanating from the "pinholes" between the fiber tows in the fabric weave. Additionally, the mixture of adhesive and prepreg resin migrated toward the cell walls, forming fillets. During this period, P_{core} rose to ~200 kPa due to ideal gas law expansion (and likely some volatile generation). During the intermediate temperature dwell, little change was observed visually, and P_{core} decayed due to continual application of vacuum to the bag.

During the second temperature ramp (between t3 and t4), the adhesive fillets appeared to "inflate" and bubbles appeared in the locations where the prepreg resin had created discontinuities in the film adhesive. After t4, all motion abruptly ceased, as the adhesive had gelled. Note that during the second temperature ramp, the adhesive viscosity was already rapidly increasing, whereas the prepreg resin was just reaching its minimum viscosity. Thus, during this ramp, bubbles could still nucleate and grow within the prepreg resin. However, they became trapped by the adhesive film. The section view of the sample in Fig. 1A confirms that the fillet "inflation" was due to the growth and entrapment of bubbles between the adhesive film and the first ply of prepreg.

Please cite the article as: Anders M, Zebrine D, Centea T, Nutt S. **Process diagnostics for co-cure of sandwich structures using in situ visualization**. Composites Part A. 2019; 116:24-35. **DOI**: 10.1016/j.compositesa.2018.09.029

P_{core} followed a similar trend during Stage III as in Stage II, first increasing during the temperature ramp (although to a lesser extent), and decaying during the dwell.

4.2. Case B

Case A showed that the continuous adhesive film was disrupted by the behavior of the prepreg resin. Specifically, the mismatch in gel times was such that, during the second temperature ramp, the prepreg resin formed bubbles that distorted – and became trapped by – the rapidly gelling adhesive layer. To prevent the adhesive from acting as a barrier for gas transport, the film was reticulated onto the core in Case B.

Fig. 7 shows P_{core} for Case B (all other temperatures and pressures are identical to Case A and thus omitted for clarity). The core evacuation during Stage I, in the absence of a continuous adhesive film, depended on the prepreg permeability. Initial evacuation was rapid, but halted as the skin compacted (analogous to the behavior observed by Kratz [20]). A new pathway for gas transport formed after ~45 min (the delay caused by gradual displacement of the highly viscous prepreg resin), allowing core evacuation to continue. During the remainder of the cycle, P_{core} followed a similar trend as in Case A, although shifted downward due to the lower initial pressure upon heating.

In Fig. 8 (Case B, t1) the reticulated adhesive is visible along the edges of the cell walls, and the first prepreg ply is visible in the center of each cell. During the room-temperature vacuum hold, minor bubble formation was observed in the adhesive and prepreg resin. As the temperature was increased between t1 and t2, the adhesive fillets formed, and a mixture of prepreg resin and bubbles could be seen pushing out from the pinholes in the fabric weave. By t2, most of the bubbles had disappeared, leaving a layer of resin at the skin/core interface and creating a continuous meniscus with the adhesive. During the dwell between t2 and t3, bubbles gradually reappeared in the prepreg

Please cite the article as: Anders M, Zebrine D, Centea T, Nutt S. **Process diagnostics for co-cure of sandwich structures using in situ visualization**. Composites Part A. 2019; 116:24-35. **DOI**: 10.1016/j.compositesa.2018.09.029

resin. During the final temperature ramp, the bubbles grew, yet none burst before resin gelation, resulting in a large cluster of bubbles at the center of each cell.

Contrasting this behavior to Case A reveals that the bubbles in the bond-line in Case A were not solely due to the adhesive acting as a barrier, but also a consequence of the core pressure. Even without the barrier (i.e., Case B), P_{core} was low enough to allow bubble growth within the resin at the skin/core interface, yet not so low that the bubbles burst. Considering this insight, the modification for Case C was chosen to afford improved control over P_{core}.

4.3. Case C

Case C simulated the conditions of a vented sandwich structure – in which P_{core} can equilibrate with P_{bag} – by connecting the core vent to the vacuum line. During the room temperature vacuum hold, thin-walled bubbles grew from the pinholes in the fabric and burst, indicating that air initially trapped between the prepreg plies was evacuating into the core. Previously, in Cases A and B, vacuum was only applied on the upper surface of the skin, so air in the core had to travel upwards through the skin to escape. Conversely, in Case C, the core was evacuated directly and simultaneously with the vacuum bag, so air was not driven through the skin, and air initially entrapped within the skin could evacuate in either direction (up through the perforations in the release film, or down into the core), along the path of least resistance.

Upon initial heating, the vacuum in the core pulled a foamy mixture of gas and resin out from the fabric pinholes. Towards the end of the first ramp (see Fig. 8, t2), vigorous frothing was observed, with large bubbles growing and bursting repeatedly. Bubble formation slowed during the intermediate-temperature dwell, but, by that point, much of the adhesive had been spattered onto the cell walls, leaving little at the skin/core interface to form fillets (see Fig. 8, t3). Small bubbles remained along the edges of the cell walls against the skin, which grew during the second

Please cite the article as: Anders M, Zebrine D, Centea T, Nutt S. **Process diagnostics for co-cure of sandwich structures using in situ visualization**. Composites Part A. 2019; 116:24-35. **DOI**: 10.1016/j.compositesa.2018.09.029

temperature ramp and became fixed at gelation (t4). The section view of this sample (Fig. 1C) provides a complementary perspective of the small, void-filled fillets and the adhesive coating the cell walls.

4.4. Case D

The staged pressure cycle used for Case D was designed to avoid the previously-observed defect formation phenomena, by applying positive pressure within the vacuum bag to suppress the release of gasses that could not be evacuated prior to gelation. Stage I was identical to Case C: reticulated adhesive and full vacuum in the bag and core, to maximize air removal from the skin while the resin and adhesive were still at high viscosity (the "equilibrated" P_{core} in Case D matched P_{bag} exactly and is omitted from Fig. 9 for clarity). During Stage II, to avoid the fillet disruption that occurred in Case C and duplicate the undisrupted flow seen in Case B, the vacuum bag was vented with N2 to ~100 kPa. To prevent excess resin exuding toward the skin/core interface, P_{auto} was increased to only 205 kPa (15 psig), maintaining the same compaction pressure ($P_{auto} - P_{bag}$) as in Stage I. Finally, in Stage III, recall that during the second temperature ramp in Cases A and B, a P_{core} range of ~50–150 kPa caused bubbles to grow yet remain sessile until gelation. In Case C, vacuum pressure in the core caused bubbles to burst, but this also caused severe fillet disruption. Therefore, in Case D, the opposite approach was used to prevent defects in Stage III: the application of positive pressure to suppress bubble formation and growth. First, P_{auto} was increased to 377 kPa (40 psig) to maintain compaction on the sample, and then P_{bag} was increased to 239 kPa (20 psig).

The images in the left column of Fig. 10 correspond to the times indicated on Fig. 9. During the initial vacuum hold, thin-walled bubbles similar to Case C appeared and burst, indicating air evacuation from the skin. During the temperature ramp and dwell of Stage II, fillet formation occurred, the flow undisrupted by bubbles (similar to Case B t2 but without the bubble formation

seen at ~50 kPa in Case B t3). The image captured at t3 for Case D (Fig. 10) was taken in the brief time after P_{auto} was increased, but before P_{core} was increased. Momentarily, resin containing small bubbles exuded from the fabric pinholes due to the increased compaction pressure. However, once the bag/core pressure was set to the final value, the excess resin receded into the skin, and the bubbles disappeared. The equal gas pressures on the upper and lower boundaries of the skin (i.e. P_{bag} and P_{core}, respectively) resulted in a hydrostatic condition in which no gas was driven through the skin. Furthermore, the gas pressure in the core/bag imposed a lower bound for the resin pressure in the skin, which prevented the formation of bubbles. The resin and adhesive remained effectively motionless during the second temperature ramp and until gelation (t4).

4.5. Case E

While the previous Case D effectively prevented porosity within the skin and fillets (see Fig. 1D), in some situations it may not be possible to use a vented sandwich structure with an equilibrated core (e.g., in marine applications where water ingress could be catastrophic). Thus, Case E was included to determine if the in-bag pressurization strategy from Case D could be effectively applied in the case of a sealed core, where gas transport must occur through the bag-side skin.

During Stage I, P_{core} rapidly approached $P_{bag,}$ but air evacuation halted as the skin compacted. Evacuation continued after a delay, similar to the behavior of Case B, although with a shorter delay time (the difference attributed to inherent variability of the materials). When the bag was vented to atmospheric pressure, P_{core} slowly started to rise, but again the rate of change of P_{core} varied spontaneously as discreet channels for airflow opened and closed. The pressure gradient across the skin reversed direction as P_{core} exceeded P_{bag} due to ideal gas law behavior, but eventually a gas pathway opened, and the two pressures equilibrated. When P_{bag} was raised at the beginning of Stage III, P_{core} rose to match it within ~90 s (>15 times faster than the equilibration at the beginning of

Please cite the article as: Anders M, Zebrine D, Centea T, Nutt S. **Process diagnostics for co-cure of sandwich structures using in situ visualization**. Composites Part A. 2019; 116:24-35. **DOI**: 10.1016/j.compositesa.2018.09.029

Stage II), suggesting that the formation of gas transport pathways through the skin was facilitated by lower resin viscosity.

The in situ observations from Case E were effectively identical to Case D. Fillet formation occurred during the first temperature ramp, and the resin/adhesive remained almost motionless from t2 until gelation, with the exception of the same momentary bleeding-then-receding of resin during the spike in compaction pressure at t3 (when P_{auto} had already been increased but P_{bag} had not).

A section view of the sample from Case E (Fig. 1E) reveals slightly more porosity within the fillets than Case D. In Case D, air was first extracted from the sample in both directions during Stage I, and when P_{core} and P_{bag} were increased during Stages II and III, P_{core} and P_{bag} were equal, so no gas was driven through the skin. Whenever a core/bag pressure difference exists, however, gas tends to tunnel through the skin by displacing liquid resin in the macro-pores of the fabric. In Case E, gas was driven through the skin, and the direction of gas flow reversed several times. Anytime the core pressure was nearing equilibrium with the bag pressure, gas traveling through the skin at that moment would have ceased to experience a pressure gradient and become stationary. Gas bubbles remaining in the bond-line upon gelation contributed to the porosity of the cured sample.

Case E illustrates how fundamentally conflicting goals render the co-cure process particularly challenging. Gas removal from the skin can prevent porosity due to entrapped air. In addition, maintaining resin pressure at the skin/core bond-line by exerting sufficient core gas pressure at the resin/gas interface can prevent void formation in the bond-line. However, evacuating the bag tends to pull gas from the core into the skin, and reduces the core pressure. Furthermore, re-pressurizing the core requires driving gas back through the skin. For this reason, co-cure with an equilibrated core is much simpler: the gas pressure in the core used to maintain resin pressure can be decoupled from the gas migration through the skin.

Please cite the article as: Anders M, Zebrine D, Centea T, Nutt S. **Process diagnostics for co-cure of sandwich structures using in situ visualization**. Composites Part A. 2019; 116:24-35. **DOI**: 10.1016/j.compositesa.2018.09.029

Lastly, the repeatability of the strategy from Case E has been tested by fabricating additional samples with identical parameters (although the full results are omitted here for brevity). Significant variability was observed in the intermittent delays in core evacuation at room temperature (e.g., compare P_{core} during Stage I for Cases B and E), which is attributed to irregularity in the size of pinholes in the fabric weave, and to variations in the alignment of pinholes between neighboring plies. However, irrespective of the extent of core evacuation during Stage I, in all tests, P_{core} reliably equilibrated with P_{bag} upon the application of elevated bag pressure at t3 (i.e., when the resin viscosity was sufficiently low that gas could displace resin rapidly). The repeatability of the core pressurization demonstrates that the in-bag pressurization strategy can be used reliably, provided that the fiber bed has sufficient permeability for the core to equilibrate before resin/adhesive gelation (for reference, plain weave prepregs similar to the one used here have been reported to have permeabilities ranging from 10−19 m2 to 10−16 m2, depending on the compaction level, resin viscosity, and saturation [21]). A facesheet consisting of unidirectional plies, for example, may preclude core pressurization – even at low resin viscosities – due to the absence of macro-pores between fiber tows. Conversely, a woven fabric with a tow width smaller than the honeycomb cell size will guarantee that each cell is connected to at least one macro-pore, increasing the likelihood that every cell can equilibrate with the externally applied gas pressure.

5. CONCLUSIONS

We have demonstrated a tool and method to directly observe bond-line formation for co-cure in realistic autoclave conditions, and presented experiments that exhibited a variety of process phenomena. Visual data acquired with this tool revealed the occurrence and timing of defect-formation mechanisms, including (a) gas entrapment by early gelation of the adhesive, (b) bond-line bubble growth at intermediate core pressure, and (c) fillet disruption from the bursting of bubbles at

Please cite the article as: Anders M, Zebrine D, Centea T, Nutt S. **Process diagnostics for co-cure of sandwich structures using in situ visualization**. Composites Part A. 2019; 116:24-35. **DOI**: 10.1016/j.compositesa.2018.09.029


low core pressures. Previous studies have speculated on the occurrence of these phenomena but, to our knowledge, this method is the first to provide in situ visual data as a function of time, temperature, and pressure. A strategy to eliminate defects via in-bag pressurization was demonstrated, and the complications associated with driving gas through the skin were explained.

The case study demonstrates the advantages of in situ visualization for composites manufacturing (specifically for autoclave co-cure, in this case). Through visual observations, the process conditions corresponding to defect formation can be identified, informed process modifications can be made, and theories about the relevant physical phenomena can be validated. Altogether, this approach can provide understanding and insight into the co-cure process that could not be attained by traditional inspection of the sandwich structures after manufacturing. Most importantly, much of the guesswork can be eliminated from process troubleshooting, and the interactions between materials and phenomena can be analyzed in realistic conditions.

Note that, while we focused on bond-line porosity as the primary quality metric, this is not the only relevant structural parameter governing mechanical performance. Sandwich components are complex structures with multiple potential failure modes, and the “weakest link” limits the overall performance (e.g., even a void-filled bond-line may be sufficiently strong such that the sandwich structure undergoes core damage before failing at the bond-line).

The tool described herein enables additional experiments worthy of investigation. Possibilities include a more detailed investigation of prepreg permeability, extension to other prepreg/adhesive/core material combinations, and process optimization for challenging cases such as thick-skinned sandwich structures. The insights gained can also inform the development of physics-based models for co-cure processes.

Please cite the article as: Anders M, Zebrine D, Centea T, Nutt S. **Process diagnostics for co-cure of sandwich structures using in situ visualization**. Composites Part A. 2019; 116:24-35. **DOI**: 10.1016/j.compositesa.2018.09.029

Acknowledgements: This work was supported by NASA NRA NNL16AA13C "A Physics-Based Process Model for Co-Cure Bonding of Honeycomb Core Sandwich Structures" and by the M. C. Gill Composites Center at the University of Southern California. The authors gratefully acknowledge helpful discussions with Dr. Jack Boyd; Armond Beal of the Gill Corporation; Suresh Advani, Pavel Simacek, and Thomas Cender of the University of Delaware; and Roberto Cano of NASA Langley Research Center. The authors are also thankful for material donations from Hexcel (Gordon Emmerson, Yen Wang), Henkel Aerospace Materials (David Leach), the Gill Corporation (Jessie MacLeod), and Airtech International (Cole Standish).

References:

1. Campbell FC. Manufacturing processes for advanced composites. London: ElsevierLtd.;2003.
2. G.C. Grimes The adhesive-honeycomb relationship Appl Polym Symp, 3 (1966), pp. 157-190.
3. F.C. Campbell, A.R. Mallow, C.E. Browning Porosity in carbon fiber composites an overview of causes J Adv Mater, 26 (1995), pp. 18-33.
4. H.-M. Hsiao, S. Lee, R. Buyny Core crush problem in the manufacturing of composite sandwich structures: mechanisms and solutions AIAA J, 44 (2006), pp. 901-907.
5. P.J. Pearce, D.R. Arnott, A. Camilleri, M.R. Kindermann, G.I. Mathys, A.R. Wilson Cause and effect of void formation during vacuum bag curing of epoxy film adhesives J Adhes Sci Technol, 12 (1998), pp. 567-584.
6. B.S. Hayes, J.C. Seferis, R.R. Edwards Self-adhesive honeycomb prepreg systems for secondary structural applications Polym Compos, 19 (1998), pp. 54-64.
7. C. Yuan, M. Li, Z. Zhang, Y. Gu Experimental investigation on the co-cure processing of honeycomb structure with self-adhesive prepreg Appl Compos Mater, 15 (2008), pp. 47-59.
8. S.M. Grove, E. Popham, M.E. Miles An investigation of the skin/core bond in honeycomb sandwich structures using statistical experimentation techniques Compos Part A Appl Sci Manuf, 37 (2006), pp. 804-812.
9. T. Hou, J.M. Baughman, T.J. Zimmerman, J.K. Sutter, J.M. Gardner Evaluation of Sandwich Structure Bonding in Out-Of-Autoclave (OOA) Processing Sampe J, 47 (2011), pp. 32-39.
10. S. Nagarajan, V.G.K. Menta, K. Chandrashekhara, T.R. Berkel, J. Sha, P. Wu, et al. Out-of-autoclave sandwich structure: processing study Sampe J, 48 (2012), pp. 24-31.
11. R.R. Butukuri, V.P. Bheemreddy, K. Chandrashekhara, T.R. Berkel, K. Rupel Evaluation of skin-core adhesion bond of out-of-autoclave honeycomb sandwich structures J Reinf Plast Compos, 31 (2012), pp. 331-339.

Please cite the article as: Anders M, Zebrine D, Centea T, Nutt S. **Process diagnostics for co-cure of sandwich structures using in situ visualization**. Composites Part A. 2019; 116:24-35. **DOI**: 10.1016/j.compositesa.2018.09.029

12. Hadsall KA, Storage KM, Storage TM, Smith JA. Evaluation and comparison of structural film adhesives for out-of-autoclave (OOA) applications using alternate cure cycles. Proc. SAMPE 2013 Conf.; 2013.
13. Anandan S, Dhaliwal GS, Chandrashekhara K, Berkel TR, Pfitzinger D. Processing and Performance of Out-of- Autoclave Bismaleimide Composite Sandwich Structures. Proc. Compos. Adv. Mater. Expo, Dallas, TX: 2015, p. October 26-29.
14. S.S. Tavares, V. Michaud, J.-A.E. Månson Through thickness air permeability of prepregs during cure Compos Part A Appl Sci Manuf, 40 (2009), pp. 1587-1596.
15. S.S. Tavares, V. Michaud, J.-A.E. Månson Assessment of semi-impregnated fabrics in honeycomb sandwich structures Compos Part A Appl Sci Manuf, 41 (2010), pp. 8-15.
16. S.S. Tavares, N. Caillet-Bois, V. Michaud, J.-A.E. Månson Non-autoclave processing of honeycomb sandwich structures: Skin through thickness air permeability during cure Compos Part A Appl Sci Manuf, 41 (2010), pp. 646-652.
17. S.S. Tavares, N. Caillet-Bois, V. Michaud, J.-A.E. Månson Vacuum-bag processing of sandwich structures: Role of honeycomb pressure level on skin–core adhesion and skin quality Compos Sci Technol, 70 (2010), pp. 797-803.
18. S. Sequeira Tavares, Y. Roulin, V. Michaud, J.-A.E. Månson Hybrid processing of thick skins for honeycomb sandwich structures Compos Sci Technol, 71 (2011), pp. 183-189.
19. J. Kratz, P. Hubert Processing out-of-autoclave honeycomb structures: Internal core pressure measurements Compos Part A Appl Sci Manuf, 42 (2011), pp. 1060-1065.
20. J. Kratz, P. Hubert Anisotropic air permeability in out-of-autoclave prepregs: Effect on honeycomb panel evacuation prior to cure Compos Part A Appl Sci Manuf, 49 (2013), pp. 179-191.
21. J. Kratz, P. HubertVacuum bag only co-bonding prepreg skins to aramid honeycomb core. Part I. Model and material properties for core pressure during processing Compos Part A Appl Sci Manuf, 72 (2015), pp. 228-238.
22. J. Kratz, P. Hubert Vacuum-bag-only co-bonding prepreg skins to aramid honeycomb core. Part II. In-situ core pressure response using embedded sensors Compos Part A Appl Sci Manuf, 72 (2015), pp. 219-227.
23. P. Davies, D. Choqueuse, G. Bourbouze Micro-tomography to study high-performance sandwich structures J Sandw Struct Mater, 13 (2011), pp. 7-21.
24. T. Centea, D. Zebrine, M. Anders, C. Elkin, S.R. Nutt Manufacturing of honeycomb core sandwich structures: film adhesive behavior versus cure pressure and temperature Proc Compos Adv Mater Expo (2016).
25. M. Anders, J. Lo, T. Centea, S.R. Nutt Eliminating volatile-induced surface porosity during resin transfer molding of a benzoxazine/epoxy blend Compos Part A Appl Sci Manuf, 84 (2016), pp. 442-454.
26. Centea T, Zebrine D, Anders M, Nutt SR. Facesheet Consolidation During Autoclave Co- Cure of Honeycomb Core Sandwich Structures. Proc. SAMPE 2017 Conf., Seattle, WA; 2017.
27. M. Anders, D. Zebrine, T. Centea, S.R. Nutt In situ observations and pressure measurements for autoclave co-cure of honeycomb core sandwich structures J Manuf Sci Eng, 139 (2017), p. 111012.
28. Hexcel Corporation. HexPly® 8552 Epoxy Matrix Properties 2013.
29. Henkel Aerospace. LOCTITE EA 9658 AERO Epoxy Film Adhesive - Technical Process Bulletin 2013.

Please cite the article as: Anders M, Zebrine D, Centea T, Nutt S. **Process diagnostics for co-cure of sandwich structures using in situ visualization**. Composites Part A. 2019; 116:24-35. **DOI**: 10.1016/j.compositesa.2018.09.029

30. Mckillen JM, Miao TY, Cornwell RE, Marsicano JM. High Strength and Durability Nacelle Film Adhesive, Hysol EA9658. Proc SAMPE 2007 Conf; 2007.
31. Reller D, Oldroyd PK. Method and Apparatus for Reticulating an Adhesive to the Surface Network of a Cellular Core Structure. US 2011/0151183. 2011.
32. Welsh JM, Popp TD, Baca LL. Method for Forming a Composite Acoustic Panel. US Patent 6,179,943 B1. 2001.
33. G. Epstein, S. Ruth Honeycomb sandwich structures: vented versus unvented designs for space systems El Segundo, CA (1993).
34. A.W. Alteneder, D.J. Renn, J.C. Seferis, R.N. Curran Processing and characterization studies of honeycomb composite structures SAMPE: Society for the Advancement of Material and Process Engineers, Anaheim, CA (1993), pp. 1034-1047.
35. R.A. Brand, G.G. Brown, E.L. McKague Processing science of epoxy resin composites GENERAL DYNAMICS SAN DIEGO CA CONVAIR DIV (1984).
36. Van Ee D, Poursartip A. NCAMP Hexply Material Properties Database for use with COMPRO CCA and Raven. 2009.

Please cite the article as: Anders M, Zebrine D, Centea T, Nutt S. **Process diagnostics for co-cure of sandwich structures using in situ visualization**. Composites Part A. 2019; 116:24-35. **DOI**: 10.1016/j.compositesa.2018.09.029